GENERATION OF RICE CROPS TEMPORAL CHANGE MAPS WITH DIFFERENTIAL TANDEM-X INTERFEROMETRY

Cristian Rossi [1] *and Esra Erten* [2]

[1] German Aerospace Center (DLR), Remote Sensing Technology Institute, Wessling, Germany.
[2] Istanbul Technical University (ITU), Geomatics Engineering, Istanbul, Turkey.

ABSTRACT

A strategy to evaluate rice plant growth from TanDEM-X data is assessed in this paper. Single fields are segmented exploiting their early vegetative stage, when they are flooded. Height is then extracted from the bistatic interferometric phase in a field-by-field basis and temporal change maps useful to production estimation are generated. The accuracy of the plant height estimation is in a decimetric level.

Index Terms— TanDEM-X, InSAR, DEM, paddy rice

1. INTRODUCTION

The use of differential interferometric phase, which is a direct function of temporal volume change, is rare in paddy rice monitoring literature. Instead, several studies have been reported for glacier, volcanoes, mining and urban area volume changes (e.g. [1]). Two aspects have to be considered in terms of monitoring applications. The first one is the potential penetration, causing an underestimation in volume deviations. The second one is the large temporal baselines, causing unreliable interferometric phase information. A promising SAR mission to attenuate these limitations is TanDEM-X [2], which allows to measure small phase center variations related to the changes in canopy height, since the relatively short X-band wavelength interacts mostly with upper sections of the crop. The objective of this work is to examine differential interferometric phase for temporal paddy rice monitoring exploring the new capabilities offered by TanDEM-X. In this paper, a stack of 16 dual-pol acquisitions over one of the largest and most productive paddy rice planting area in Turkey, around Gala lake, is analyzed. A separated ground truth GPS campaign is also performed and used to validate the interferometric heights [3, 4].

2. INPUT DATA

In the framework of the German Aerospace Center (DLR) project $XTILAND1476$, 16 dual-pol TanDEM-X acquisitions have been acquired over the Gala lake region in 2012 and 2013. Specifically, 9 acquisitions have been commanded in 2012 and 8 in 2013 at the same incidence angle. As shown in Table I, only the 2012 acquisitions are covering all the rice growing stages (May to October), whereas the 2013 acquisitions are missing the maturation stage (August to October). For this reason, even though the GPS campaign has been conducted in 2013, the sole 2012 acquisitions are employed in the following analysis. An additional reason relies to the height sensitivity of the different bistatic configurations. Height of Ambiguity (HoA), an important system parameter describing the elevation range of a phase cycle - smaller it is more accurate the generated DEM -, is ranging between about 20 and 30 meters for the 2012 acquisitions and between about 40 and 50 meters for the 2013 ones. To give a quantitative idea, assuming a Gaussian distributed phase error, a coherence value of 0.8 yields a standard error of 0.36 meters for the 12.05.2012 processed configuration (HoA: 23.1 m) and a standard error of 0.84 meters for the 26.07.2013 one (HoA: 52.8 m) (see last column in Table I).

The data stack is processed with the Integrated TanDEM-X Processor (ITP) at the DLR processing facilities [2]. ITP is the operational system employed in the TanDEM-X mission for the generation of the raw DEM given as input SAR raw data. The processor is commanded to generate HH and VV DEMs, for a total of 32 DEMs, with an output raster of 6 meters. As in Table I, the interferogram resolution is triggered to be around 10 meters by multi-looking the input co-registered data. Considering the purpose of tracking crop height in all the growing stages, multi-looking process is a necessary step to reduce the phase noise and the resulting standard error to a decimetric level. Due to the relatively smooth topography of the scenes, phase unwrapping is not an issue (even for small height of ambiguities) and no unwrapping errors have been detected. To ensure a straightforward analysis, all the DEMs have been generated at the same output grid and have been equally calibrated jointly using SRTM and ICESat data. For the following analysis, the HH channel has been chosen. A study with the differences observed between the different polarizations is provided in [4].

Table 1. MAIN PARAMETERS OF THE INTERFEROMETRIC DATA SET (HH CHANNEL)

acquisition date (DOY)		center incidence angle [deg]	perpendicular baseline [m]	height of ambiguity [m]	interferogram resolution [m]	mean coherence	standard error [m]
12.05.2012	(133)	36.8	253.7	23.1	10.2	0.82	0.36
14.06.2012	(166)	36.8	242.3	24.2	10.3	0.80	0.38
06.07.2012	(188)	36.8	234.3	25.1	10.2	0.84	0.40
17.07.2012	(199)	36.8	227.2	25.8	10.2	0.82	0.41
28.07.2012	(210)	36.8	222.7	26.3	10.3	0.83	0.42
19.08.2012	(232)	36.8	213.4	27.4	10.2	0.83	0.43
10.09.2012	(254)	36.8	204.4	28.7	10.3	0.82	0.46
13.10.2012	(297)	36.8	187.1	31.3	10.3	0.84	0.50
26.11.2012	(331)	36.8	181.3	32.3	10.3	0.84	0.51
05.03.2013	(64)	36.8	112.0	52.8	10.4	0.76	0.83
16.03.2013	(75)	36.8	111.5	53.1	10.4	0.80	0.84
10.05.2013	(130)	36.8	139.7	42.1	10.4	0.84	0.67
21.05.2013	(141)	36.8	141.1	41.6	10.3	0.81	0.66
01.06.2013	(152)	36.8	146.6	40.2	10.3	0.78	0.63
23.06.2013	(174)	36.8	144.3	40.7	10.4	0.85	0.64
26.07.2013	(207)	36.8	111.6	52.8	10.3	0.85	0.84

* Standard error computed at a coherence value of 0.8.

3. PROCESSING STRATEGIES

The main scope of the interferometric investigation is the verification of rice stages by using temporal elevation data. To this aim, field segmentation is mandatory, reasonably assuming a consistent growing within single fields. An important sub-product to exploit, generated during the interferometric processing, is the coherence. By describing the similarity of the coregistered complex master and slave data, the coherence is a considerable input for the analysis, supporting the segmentation algorithm. Flooded parcels of land characterize the early vegetative paddy rice state. During this state, fields are covered by water and separated by a path network composed by soil or rare grass. A gravel road network is also in the test site separating parcel groups. This natural segmentation is well visible by inspecting the 12.05.13 interferometric coherence in Fig. 2, as good as inspecting the master channel amplitude in Fig. 1. This visibility relies on the water body electromagnetic spectrum. Non-moving water behaves like a mirror, reflecting the incident signal wave in a specular direction, yielding a very low return to the SAR antenna. This phenomenon brings also a low interferometric coherence due to the consequent SNR decorrelation. Moreover, it is also known that a water body decorrelates within tens of milliseconds [5]. Although TanDEM-X is a bistatic mission built to avoid temporal decorrelations, the satellites formation brings small along-track time lags varying between 50 ms (equator) and 0 ms (poles). The global study performed in [6] demonstrated that from 10 ms water decorrelates. In the studied test case, the mean measured time lag of about 30 ms overcomes the limit. Several investigations have been proposed about the derivation of water bodies from the joint use of amplitude and coherence. In this paper the technique proposed by [6], operationally employed for the generation of water body mask as an auxiliary product of the official TanDEM-X DEM, is adopted. By analyzing 1700 randomly worldwide-distributed scenes, [6] established two thresholds that provided a correctness analysis well above 90 %. Specifically, a threshold value of 40 for the amplitude digital number (corresponding to -18 dB in radar brightness and about -20 dB in Sigma-Nought for the studied case) and 0.23 for the coherence were selected. Three water mask confidence levels are then generated: (1) detection from coherence threshold, (2) detection from amplitude threshold and (3) detection from both thresholds. The third level represents the highest confidence one. In this study, this strategy is applied for scenes having flooded crops. In Fig. 1 and Fig. 2, the 12.05.2012 amplitude and coherence data show the flooded parcels for that date with low values. As visible, not all the fields were already flooded. To better cover the test site, additional information is retrieved by using also the 21.05.2013 and 01.06.2013 acquisitions.

A potential issue in the detection relies in the presence of wind during the acquisition. For the Rayleigh criterion, a surface is regarded as specular if its vertical variation is smaller than about 5 mm for X-band at 36.8 deg. Wind may induce waves with height well above this value resulting in backscattered energy at the sensors. Thus, amplitude threshold can result too low for these cases and can generate misdetections. Nevertheless, water decorrelation yields low coherence and water results masked with the second confidence level. In the study area, the highest confidence level is reached for all the detections indicating a proper threshold selection for both

Fig. 1. SAR master channel amplitude of the 12.05.2012 TanDEM-X acquisition, used to extract field shapes.

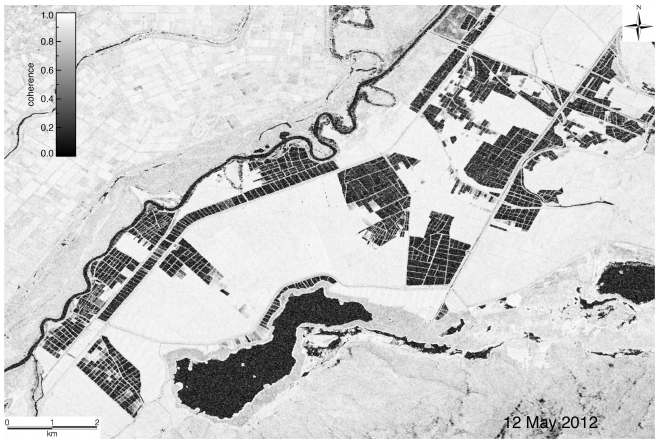

Fig. 2. Interferometric coherence of the 12.05.2012 TanDEM-X acquisition, used to extract field shapes.

amplitude and coherence.

Straight after the water detection, a binary morphological erosion with a $3-by-3$ rectangular structuring element is performed to remove isolated artifacts and a binary shape fill is performed to remove possibly remaining holes within shapes. The final mask is then segmented and the fields numbered. A total of more than 2000 fields are detected. The detection and the segmentation are performed in the geocoded domain, in order to easily compare them with ground truth data. To be noticed, geolocation errors hardly occur due to the precise calibration and the practically flat scenario.

Fig. 5 shows the mean 2012 coherence values for detected flooded fields on 12.05.2012 (red points) and the mean 2013 values for fields flooded on 21.05.2013 (green points). The 2012 acquisitions, spanning the plant growing cycle, exhibit the good quality of the derived elevation for all the

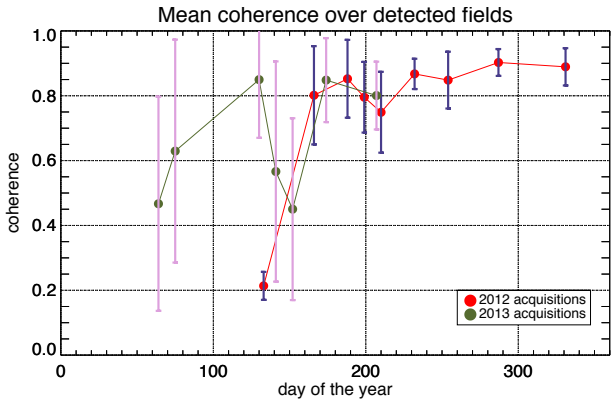

Fig. 3. Mean coherence trend for the fields extracted by using the 12.05.2012 acquisition (red line) and by using the 21.05.2013 acquisition (green line). The standard deviation is highlighted with error bars.

stages (June-September) excluding the early vegetative stage (May). A coherence of around 0.2 for the May acquisition (flooded field) yields not reliable elevation values. Moreover, this value results overestimated due to the estimation bias caused by the finite estimation support of 11 by 11 samples [5]. Accurate heights are instead generated for the later data. Coherence fluctuates around 0.8 for the June-July data with a decreasing trend mainly caused by the increasing height of ambiguity for similar field conditions (wet environment, fresh plants). This value increases for the following two acquisitions (August-September) as the field condition switches to dense vegetation, ideally behaving like a distributed scatterer. To be noticed, a coherence value of around 0.85 corresponds to better height accuracy than the one specified in Table I. The last two 2012 acquisitions are over the plant cycle, after the harvesting. Here, coherence around 0.9 indicates very accurate elevation values, as the field condition transformed to bare soil with a very rough surface yielding high SNR. The last acquisition, November 2012, is taken as reference as indicates the terrain height without water or rice plants. The 2013 acquisition are also showed in Fig. 5 for completeness. The first two data cover the early-year period prior the plantation and have huge coherence variations, also denoting poor elevation accuracy. The field detection is performed for the late May acquisition, showing a similar value and accuracy to the one used for the 2012 field extraction. The prior and following data provide a higher coherence with high variations, indicating non-homogeneous conditions for the fields under analysis. The last two acquisitions, in the reproductive stage, follow the same trend of the 2012 one.

Fig. 4 and Fig. 5 visually shows the plant growth of July 06 and August 19, 2012, respectively. The differences with the reference height of November 2012 are here represented with an overlay between the amplitude and the mean height

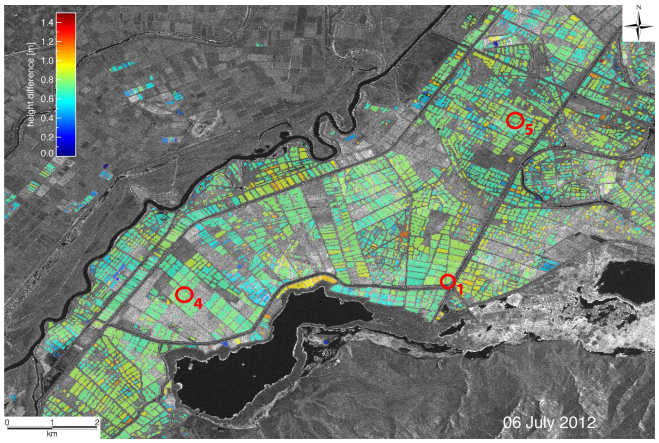

Fig. 4. Temporal 2012 height change analysis. Difference between the 06.07 and the reference 26.11 acquisitions.

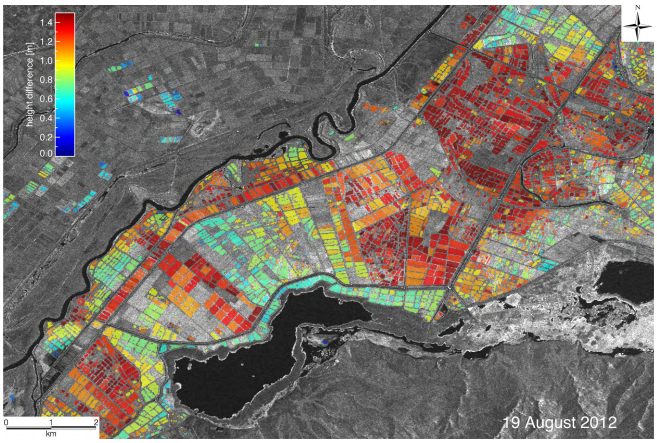

Fig. 5. Temporal 2012 height change analysis. Difference between the 19.08 and the reference 26.11 acquisitions.

difference for all the detected fields having an average coherence above 0.8 for both the analyzed and the reference acquisitions. Inspecting these maps, one could check the growing trend on a field-by-field basis. For instance, the July map in Fig. 4 shows a quite homogeneous result with plant heights around 70 cm. The August map in Fig. 5 reveals the growing of most of the plants, with doubled heights in average. In general, these maps can be used for the agricultural planning, in terms of production volume and outcomes.

Finally, to highlight the TanDEM-X capability in assessing the temporal crop growth, in Fig. 6 the mean height for the 2012 detected fields (flooded in Fig. 1) is shown in black and the standard deviation highlighted in purple. The reference temporal elevation is over-plotted. Although a detailed validation is provided in [4], by using eight reference fields as shown in the figure, the mean trend already shows a good accordance with the reference, with decimetric errors. The height deviation for the late July acquisitions has to be linked to the different growing periods of the detected fields.

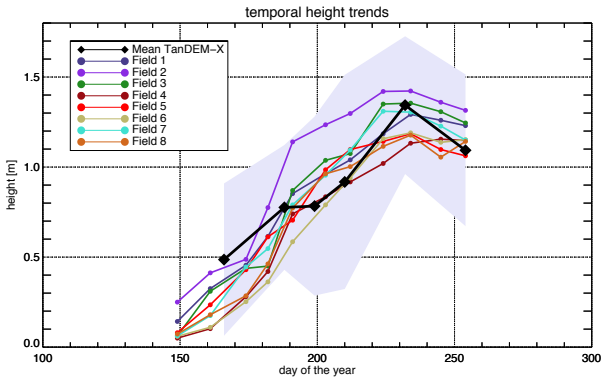

Fig. 6. Mean temporal TanDEM-X elevation trend for 2012 detected fields (black) and corresponding standard deviation (purple). The reference fields are overplotted with colors in the legend.

The Rice and Wetlands monitoring in Turkey project is performed by funding of The Scientific and Technological Research Counsil of Turkey (TUBITAK project no: 113Y446). TanDEM-X SAR data were supplied by German Aerospace Center under the project no:XTILAND1476.

4. REFERENCES

[1] M. Eineder, T. Fritz, W. Abdel Jaber, C. Rossi, and H. Breit, "Decadal Earth Topography Dynamics Measured with TanDEM-X and SRTM," in Geoscience and Remote Sensing Symposium 2012 (IGARSS), pp. 1916-1919., 2012.

[2] C. Rossi, F. R. Gonzales, T. Fritz, N. Yague-Martinez, and M. Eineder, "TanDEM-X Calibrated Raw DEM Generation," *ISPRS Journal of Photogrammetry and Remote Sensing*, vol. 73, pp. 1220, 2012.

[3] E. Erten, C. Rossi, O. Yuzugullu and I. Hajnsek, "Phenological Growth Stages of Paddy Rice According to the BBCH Scale and SAR Images," in Geoscience and Remote Sensing Symposium 2014 (IGARSS).

[4] C. Rossi and E. Erten, "Paddy Rice Monitoring with TanDEM-X" *Geoscience and Remote Sensing, IEEE Trans. on*, submitted.

[5] R. Bamler and P. Hartl, "Synthetic aperture radar interferometry," *Inverse problems*, vol. 14, no. 4, 1998.

[6] A. Wendleder, B. Wessel, A. Roth, M. Breunig, K. Martin, S.Wagenbrenner, "TanDEM-X Water Indication Mask: Generation and First Evaluation Results," *Selected Topics in Applied Earth Observations and Remote Sensing, IEEE Journal of*, vol.6, no.1, pp.171,179, Feb. 2013.